

## Article

# Hydrochemical Characteristics and Ion Sources of Soil-Soluble Salt in the Water-Level Fluctuation Zone of the Lower Jinsha River Basin

Ke Jin <sup>1,\*</sup>, Qianzhu Zhang <sup>1</sup>, Jiang Yu <sup>2</sup>, Yang Lu <sup>1</sup>, Huoming Zhou <sup>1</sup>, Dan Wan <sup>1</sup>, Cha Zhao <sup>1</sup> and Yue Hu <sup>1</sup><sup>1</sup> Chongqing Branch, Changjiang River Scientific Research Institute, Chongqing 400026, China<sup>2</sup> Environmental Protection Department of China, Three Gorges Projects Development Co., Ltd., Chengdu 610023, China

\* Correspondence: jin55669987@163.com

**Abstract:** The water-level fluctuation zone of the lower Jinsha River Basin is a fragile ecosystem with limited water resources in the southwest of China. Soil water is critical for maintaining ecological balance and promoting the healthy development of animals and plants in this region. In this study, eight typical soil profiles were monitored for hydrochemistry in soil-soluble salt from upstream to downstream of the lower Jinsha River Basin. The results show that the soil water content was low and had a negative correlation coefficient with major ions in the soil-soluble phase. The soil-soluble salt is slightly alkaline, and  $\text{Ca}^{2+}$ ,  $\text{Na}^+$ ,  $\text{SO}_4^{2-}$ , and  $\text{HCO}_3^-$  are important components for ions in a soluble phase. Major ions in soluble salt originate from various sources, including precipitation, anthropogenic input, silicate weathering, and carbonate weathering, and the contribution rates from each end member were 0.7%, 45.1%, 25.2%, and 29%, respectively. The ion composition in surface soil soluble salt is mainly influenced by precipitation and human activities, while the ions in the 0–50 cm soil layer originate from the precipitation input and water-rock interaction. In addition, rock weathering is a vital process for releasing ions into soil-soluble salt from 50 to 100 cm soil layer. Our findings provide important references for ion sources and the eco-hydrological process in limited water resources in the water-level fluctuation zone of the lower Jinsha River Basin.

**Keywords:** soil-soluble salt; hydrochemistry; ion sources; rock weathering; lower Jinsha River Basin

**Citation:** Jin, K.; Zhang, Q.; Yu, J.; Lu, Y.; Zhou, H.; Wan, D.; Zhao, C.; Hu, Y. Hydrochemical Characteristics and Ion Sources of Soil-Soluble Salt in the Water-Level Fluctuation Zone of the Lower Jinsha River Basin. *Water* **2023**, *15*, 1403. <https://doi.org/10.3390/w15071403>

Academic Editor: Aldo Fiori

Received: 23 February 2023

Revised: 30 March 2023

Accepted: 31 March 2023

Published: 4 April 2023



**Copyright:** © 2023 by the authors. Licensee MDPI, Basel, Switzerland. This article is an open access article distributed under the terms and conditions of the Creative Commons Attribution (CC BY) license (<https://creativecommons.org/licenses/by/4.0/>).

## 1. Introduction

Soil water plays an important role in water-limited areas such as semi-arid and arid areas, which cover more than 40% of the land's surface worldwide [1]. The ecosystems are exceedingly fragile, with rare precipitation and strong evaporation in water-limited areas. Soil water is a significant component of the hydrological cycle, which strongly influences the water and energy dynamics at the surface-atmosphere interface [2]. Particularly, the dry hot valley is one of the ecologically fragile zones and is a special arid area around the world [3]. Since the climate in the dry hot valley is the main limiting factor for vegetation restoration and reconstruction, the characteristics of soil water infiltration are very important to improve the effectiveness of vegetation restoration, alleviate soil degradation, and maintain the stability of the ecosystem in this region [4].

The Jinsha River Basin is an ecological security barrier in the upper reaches of the Yangtze River and is an important hydropower base in China. The lower Jinsha River Basin is a typical dry-hot valley zone with drought and rare rain, prominent water heat contradictions, and serious vegetation degradation. Although the ecological environment is extremely fragile, abundant hydropower resources can support and construct 4 hydropower stations for power generation, flood control, and shipping. However, it also leads to the formation of water-level fluctuation zones along the reservoir due to the periodic fluctuation of the water level in this region. The water-level fluctuation zone is a special transition zone

with the alternation of wetting and drying, which plays an important role in vegetation restoration, soil erosion, and pollutant cycling [5–7]. The extreme climate and reservoir water regulation have a serious influence on the distribution and exchange of limited water resources in the water-level fluctuation zone of the Jinsha River Basin. Soil water can provide necessary water sources and important nutrients for plant growth and is the core of the water cycle in the water-level fluctuation zone of the Jinsha River Basin.

Soil moisture is influenced by many factors, such as altitude, soil type, land use type, rainfall, and evaporation intensity in the dry-hot valley [3]. In addition, soil moisture is influenced by the catchment area and runoff in the rainy season, while the soil characteristics, vegetation types, and microtopography can control the distribution of soil moisture in the dry season [8]. Many researchers have studied the variation characteristics of soil moisture, influence factors, and recharge sources in the dry-hot valley of the Jinsha River Basin. For instance, Yue et al. [9] found that the soil moisture content increases along the soil depth, and the moisture content in the rainy season is obviously higher than that in the dry season. Some researchers thought that soil moisture had a significant spatial structure and continuity, and it also had a similar spatial autocorrelation in different dry and rainy seasons under different forest and grass vegetation in this region [10]. Some suggested that the seasonal change in soil moisture was mainly affected by the seasonal change in climate factors such as precipitation, temperature, light intensity, and evaporation [11]. Furthermore, vegetation cover plays an important role in impacting the distribution of soil moisture in the Jinsha River Basin. The Silver wattle forest can effectively reduce water evaporation in a 0–40 cm soil layer during the rainy season, playing a key role in water and soil conservation [12]. Although many achievements with soil moisture have been made in the dry-hot valley of the Jinsha River Basin, the hydrochemical characteristics and ion sources of soil-soluble salt in the water-level fluctuation zone have been poorly understood until now.

Many traditional methods have been applied to analyze the distribution, recharge source, and movement of soil water, such as intensive observation, hydrologic experiments, isotopic tracing, and remote sensing [13–15]. Specifically, hydrochemistry methods not only play a key role in determining water quality and its controlling mechanisms but also facilitate exploring the water-rock interaction and cation exchange [16,17]. It is also very useful for studying the chemical evolution and weathering of soils in arid regions using hydrochemistry analysis [18]. For example, the evaporation effect and accumulation patterns in the soil profile of a northern desert have been discussed through the use of  $\text{Cl}^-$  and  $\text{SO}_4^{2-}$  ionic tracing [19]. Tan et al. [20] used the Cl contents to discuss the infiltration mechanism of soil water at different times and explored the migration process of soil water in high loess hills on the Loess Plateau. Jin et al. [21] used hydrochemistry methods to research the recharge source and chemical weathering of the soil-soluble phase in an arid area. Therefore, such methods can be used for studying the distribution and chemical process of soil-soluble salt in the water-level fluctuation zone of the Jinsha River Basin.

In this study, we investigated the hydrochemical composition of soil-soluble salt in the water-level fluctuation zone from eight typical soil profiles in the Wudongde reservoir and Baihetan reservoir of the lower Jinsha River Basin. The objectives of this study were (1) to identify the distribution characteristics of ions in the soil-soluble phase and their impact factors and (2) to evaluate the chemical weathering and contribution rate from potential sources for soil-soluble salt in the water-level fluctuation zone in this region. Our findings could be helpful for understanding water distribution and ion sources of soil-soluble salt in the water-level fluctuation zone of the lower Jinsha River Basin.

## 2. Study Area

The Jinsha River Basin is in the upper reaches of the Yangtze River, which flows between Sichuan, Tibet, and Yunnan provinces. The mainstream is 3481 km, the drainage area is about  $5 \times 10^4 \text{ km}^2$  which accounts for 27.8% of the total area of the Yangtze River Basin, and the total altitude difference is more than 5000 m [22]. The downstream of the

Jinsha River, located at the junction of Sichuan and Yunnan provinces, is from Panzhihua city to Yibin city, and its total length is about 782 km. It is an important hydropower base in China and lies within 25°00' N, 101°00' E and 29°00' N, 105°00' E (Figure 1). There are four hydropower stations the downstream of Jinsha River Basin named the Wudongde, the Baihetan, the Xiluodu, and the Xiangjiaba, among which the Wudongde hydropower station and Baihetan hydropower station are the first and second steps in these regions.

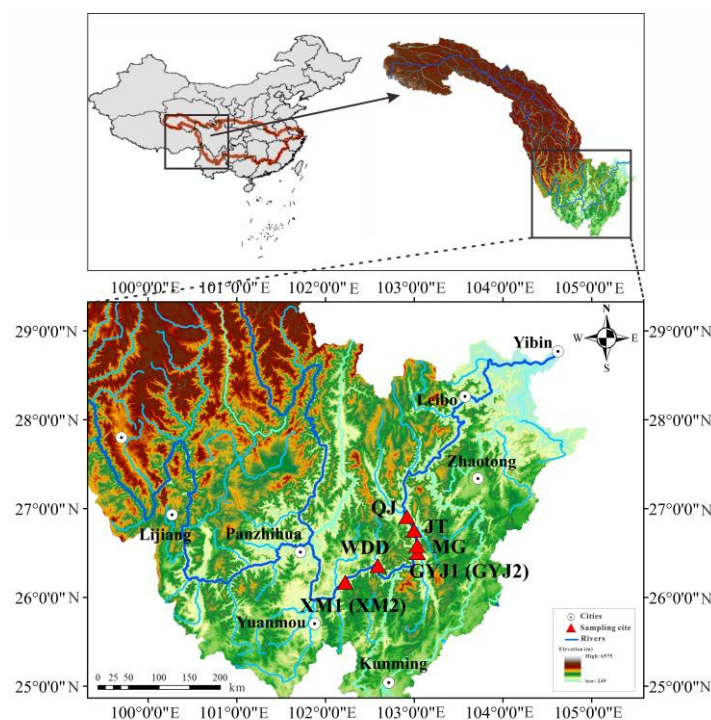


**Figure 1.** Map showing the study area and sampling locations.

The lower Jinsha River Basin belongs to a typical dry-hot valley climate. The annual rainfall is only 600~800 mm, and most of the rainfall is concentrated in the rainy season (May to October); while the precipitation is extreme, it accounts for only 10% of the annual rainfall in the dry season (November to April) [23]. The annual potential evaporation is 3850 mm, and the evaporation in the dry season is 27 times the precipitation in the same period. The annual average temperature is 20~27 °C in this region [24]. The vegetation community structure is simple and unstable, and most of the plants are mainly herbs. The dominant species include *Heteropogon contortus*, *Bothriochloa pertus*, *Dodonaea viscosa*, *Vitex negundo* L., *f.laxipaniculata* Pei, *Phyllanthus emblica*, and *Bombax ceiba* in the dry-hot valley [25]. There are two restoration modes named ecological restoration areas and natural recovery areas for the water-level fluctuation zone in this region. Only two sites were selected for ecological restoration in the Wudongde reservoir (WDDR) and Baihetetan reservoir (BHTR), respectively. Both the ecological restoration areas are about 0.2 km<sup>2</sup> with a 3 km length along the shoreline in the WDDR and the BHTR. The recovery time for the two modes is about 3 years (WDDR) and 2 years (BHTR), respectively, while the natural recovery time of the water-level fluctuation zone in the Xiluodu and Xiangjiaba reservoirs is more than 10 years. The main soil types are torrid red soil, mountain red soil, yellow-brown, and brown soil in the dry-hot valley [26]. Meanwhile, most of the soils belong to loam and serve as tillage in the water-level fluctuation zone of the lower Jinsha River Basin. The main plant species are *Leucaena leucocephala* (Lam.) de Wit, *Morus alba* L., *Dodonaea viscosa* Jacquem, and *Heteropogon contortus* in natural recovery areas of the water-level fluctuation zone, while the flooding resistance species (i.e., *Taxpidium ascendens*, *Salix variegates*, and *Cynodon dactylon*) are mainly distributed in the ecological restoration areas in this region. Some agricultural activities (i.e., fertilization and watering) and sewage

discharge were found in the ecological restoration areas, but almost none were found in the natural recovery areas during the field investigation.

### 3. Materials and Methods

#### 3.1. Soil Samples Sampling

Eight soil profiles located at the water-level fluctuation zone in six typical regions were sampled in the lower Jinsha River Basin in July 2022 (Figure 1). At this time, the water-level fluctuation zone was not inundated due to the off-season fluctuation rhythm of the reservoir, and all the samples were collected in the rainy season for analyzing the ions composition and sources for soil-soluble salt. Two soil profiles (each, i.e., XM1/XM2 and GYJ1/GYJ2) were monitored in the ecological restoration areas of the WDDR and the BHTR, respectively, while others were surveyed in the natural recovery areas of the WDDR and the BHTR. Three soil profiles were sampled at the WDDR, which were named XM1, XM2, and WDD from upstream to downstream, while five soil profiles were sampled in the BHTR and named GYJ1, GYJ2, MG, JT, and QJ from upstream to downstream (Figure 1). All the soil profiles were generally drilled with a depth of 100 cm using a hollow-stem hand auger for the collection of soil samples. Bulk soil samples were collected at an interval of 10 cm, and each sample was separated into two parts. One was approximately 100 g and was sealed in aluminum boxes that had been pre-weighed and immediately moved to a tent to analyze the gravimetric moisture content using a high precision balance. The other was about 500 g, which was sealed in airtight polyethylene bottles to prevent evaporation and contamination for hydrochemistry analysis.

#### 3.2. Analysis of Hydrochemistry Method

The whole soil samples were dried at 105 °C for 24 h in the laboratory in order to determine the gravimetric moisture content based on the difference between bulk and dry weights. To analyze the ionic concentrations of soil-soluble salt, 100 g of dried soil with the addition of 200 mL Milli-Q water was shaken for 24 h in each sample. Then, the supernatant solution was separated using a centrifuge and filtered through 0.45 µm filters. The filtered soil solution was stored in two parts; one was stored without further treatment in a 15 mL tube for anion measurement, and the other was acidified with ultra-pure nitric acid to a pH value of about 2 for cation measurement. The major cations were measured by a plasma spectrometer (ICP-7000), and the measurement of the major anions was conducted by ionic chromatography (ICS-600) at the Changjiang River Scientific Research Institute. Reagent and procedural blanks were analyzed in parallel to the sample treatments using identical procedures. The analytical error was 5% for cations and 3% for anions based on the sample reproducibility. Additionally, the  $\text{HCO}_3^-$  was measured by the HCl titration with a precision of 3% within 24 h of supernatant solution collection.

#### 3.3. Hydrochemical Analysis

The hydrochemical properties and processes (i.e., evaporation, precipitation, and water-rock interactions) of soil-soluble salt could be presented in Piper plots and Gibbs plots [27,28], respectively. Additionally, it often used the bivariate diagrams of different ions to determine the hydrochemical properties and solute sources of various water [29].

The chloro-alkaline indices have been widely used to explore the possibility of cation exchange between the water and its surrounding environment [30]. In this study, the two indices were calculated as follows [31]:

$$\text{CAI-1} = 1 - (\text{Na}^+ + \text{K}^+)/\text{Cl}^- \quad (1)$$

$$\text{CAI-2} = [\text{Cl}^- - (\text{Na}^+ + \text{K}^+)]/(\text{SO}_4^{2-} + \text{NO}_3^- + \text{HCO}_3^-) \quad (2)$$

The principal component analysis is also useful for identifying significant factors affecting the hydrochemistry of major ions in the soil [29]. This study presents an assessment by

selecting two factors with eigenvalues greater than one. In order to assess the contribution rates of each potential ion source for soil-soluble salt in the water-level fluctuation zone of the lower Jinsha River Basin, we established a mass balance equation as follows:

$$[X]_{\text{sss}} = [X]_{\text{pre}} + [X]_{\text{ant}} + [X]_{\text{sil}} + [X]_{\text{car}} \tag{3}$$

where  $[X]_{\text{sss}}$  refers to the total ion concentration in soil-soluble salt, and the subscripts pre, ant, sil, and car represent the ions from the precipitation, anthropogenic activities, silicate weathering, and carbonate weathering, respectively.

The ion contribution to the soil-soluble salt from precipitation can be calculated as follows [29]:

$$[X]_{\text{pre}} = (X/Cl)_{\text{pre}} \times [Cl]_{\text{pre}} \tag{4}$$

where  $[X]_{\text{pre}}$  is the corrected ion input for soil-soluble salt from precipitation,  $[Cl]_{\text{pre}}$  is the  $Cl^-$  concentration in precipitation, and the  $(X/Cl)_{\text{pre}}$  is the molar ratio between major ions and  $Cl^-$ .

#### 4. Results

The chemistry results of soil-soluble salt are provided in Table S1 and statistically listed in Table 1. The soil water content (SWC) is low in the water-level fluctuation zone of the lower Jinsha River Basin, and the mean value of soil water content was 10.09% and 9.19%, respectively, for soil profiles in the WDDR and the BHTR (Table 1). The soil water content of soils in the ecological restoration areas was lower than that in natural recovery areas with the water-level fluctuation zone. In detail, the soil water content of soils (XM1 and XM2) was about 6% in the ecological restoration areas, which is lower than the soils (WDD) and the mean value of 17.78% in the natural recovery areas of the WDDR (Table 1). Similar to the soils in the WDDR, the soils have lower SWC with a mean value of 5.12% in ecological restoration areas while also having higher SWC with an average value of 11.9% in the natural recovery areas in the BHTR (Table 1). The SWC is lower in ecological restoration areas due to more plants that are needed to supply water for growth. From the surface to the bottom of soil profiles, the soil water content shows an increasing trend. The soil water content of surface samples was averaged for 5.24%, with a mean value of 8.07% and 11.55%, respectively, for the soil samples in the 0–50 cm and 50–100 cm depth of the soil profiles in this region (Table S1). The vertical variation characteristics of the soil water content were similar between the soils in the WDDR and the BHTR. In detail, the SWC of surface soil samples was similar to that collected from the WDDR (5.38%) and the BHTR (5.15%). Additionally, the SWC of soils in 0–50 cm collected from the BHTR was higher but lower for soils in 50–100 cm than that in the WDDR (Table S1).

**Table 1.** Statistical summary of pH, EC values and ion concentrations of soil-soluble salt in the study area (the unit of EC is mS/cm, the unit of soil water content is %, and the unit of ion concentration is mg/L).

Location	Site	Altitude	Value	SWC	pH	EC	K <sup>+</sup>	Na <sup>+</sup>	Ca <sup>2+</sup>	Mg <sup>2+</sup>	Cl <sup>-</sup>	NO <sub>3</sub> <sup>-</sup>	SO <sub>4</sub> <sup>2-</sup>	HCO <sub>3</sub> <sup>-</sup>
WDDR restoration	XM1	971 m	Min.	3.71	7.26	4.49	36	116	304	81	109	52	263	407
			Max.	8.24	8.00	30.96	270	802	3443	801	1548	103	3826	3955
			Mean	6.30	7.71	14.56	78	331	1341	352	429	82	1052	1349
			Median	6.22	7.67	11.47	59	265	1005	277	357	81	734	945
			SD	1.54	0.25	8.62	69	221	993	230	407	19	1023	1036
	XM2	974 m	Min.	4.62	8.00	5.18	43	130	479	31	45	72	182	569
			Max.	7.00	8.49	10.83	145	285	1000	162	167	221	470	1191
			Mean	6.19	8.32	7.23	60	215	644	58	97	96	323	757
			Median	6.10	8.41	7.05	50	223	621	47	91	82	325	715
			SD	0.72	0.18	1.46	30	50	140	38	40	45	109	172

Table 1. Cont.

Location	Site	Altitude	Value	SWC	pH	EC	K <sup>+</sup>	Na <sup>+</sup>	Ca <sup>2+</sup>	Mg <sup>2+</sup>	Cl <sup>-</sup>	NO <sub>3</sub> <sup>-</sup>	SO <sub>4</sub> <sup>2-</sup>	HCO <sub>3</sub> <sup>-</sup>
WDDR recovery	WDD	959 m	Min.	7.17	7.81	1.99	6	68	133	32	49	39	331	76
			Max.	29.73	8.20	10.29	123	303	928	202	158	351	1184	816
			Mean	17.78	7.98	4.75	25	158	398	99	79	130	720	303
			Median	15.98	7.97	4.20	16	162	335	90	66	85	681	196
			SD	9.10	0.11	2.55	35	70	249	55	32	112	286	257
BHTR restoration	GYJ1	812 m	Min.	0.74	7.91	10.53	114	414	714	124	287	116	635	520
			Max.	6.54	8.25	41.67	2789	2017	2865	537	1833	806	6321	4373
			Mean	3.63	8.03	19.78	441	764	1296	235	832	430	2287	1288
			Median	3.43	8.00	17.16	194	617	1165	207	681	474	1638	1023
			SD	1.69	0.11	9.41	826	452	652	122	535	229	1736	1137
	GYJ2	820 m	Min.	4.08	7.90	4.52	75	71	327	99	82	67	297	355
			Max.	10.06	8.32	19.74	227	213	1763	421	551	334	4475	1026
			Mean	6.61	8.08	9.13	129	144	706	194	191	152	1419	612
			Median	6.31	8.11	7.63	110	150	569	160	157	117	1221	549
			SD	1.93	0.14	4.47	54	48	427	95	135	98	1211	263
BHTR recovery	MG	806 m	Min.	8.14	7.82	2.65	49	34	222	40	43	80	178	193
			Max.	15.51	8.22	4.93	109	125	417	72	101	210	336	521
			Mean	12.51	8.00	3.34	65	62	277	51	82	149	226	280
			Median	13.70	7.99	2.94	55	50	250	47	84	151	209	233
			SD	2.90	0.12	0.78	20	30	64	11	17	35	51	105
	JT	819 m	Min.	8.74	7.99	1.98	54	16	126	26	49	46	239	131
			Max.	15.50	8.42	7.49	105	49	790	128	106	164	1180	661
			Mean	13.33	8.25	3.60	67	28	324	53	70	88	382	276
			Median	14.41	8.25	2.79	58	23	238	36	70	70	267	195
			SD	2.49	0.14	1.81	19	12	213	37	15	40	295	177
QJ	810 m	Min.	3.11	8.33	3.18	68	54	198	59	61	33	148	298	
		Max.	14.19	8.55	16.36	348	376	1065	213	284	148	727	1702	
		Mean	9.86	8.44	5.95	121	124	371	95	178	65	289	562	
		Median	10.79	8.44	4.56	88	88	273	81	191	50	214	403	
		SD	3.54	0.08	3.91	85	98	258	47	88	37	167	424	

All soil-soluble salt is slightly alkaline; the pH value varied from 7.26 to 8.49 with a mean value of 8 in the WDDR, while the pH valued between 7.82 and 8.55 with a mean value of 8.16 in the BHTR (Table 1). The EC values varied from 1.99 to 30.96 mS/cm with a mean value of 8.84 mS/cm in the WDDR, and the EC value changed between 1.98 mS/cm and 41.67 mS/cm with an average value of 8.36 mS/cm in the BHTR (Table 1). The pH of soil-soluble salt was lower for soils (i.e., XM1, XM2, GYJ1, and GYJ2) in the ecological restoration areas than those (i.e., WDD, MG, JT, and QJ) in the natural recovery areas, while the soils in the ecological restoration areas had higher ECs than those in the natural recovery areas in the lower Jinsha River (Table 1 and Figure 2b,c). The pH of soil-soluble salt in different soils layer had no obvious variation, while the EC gradually decreased from the surface to the bottom of soil profiles (Table S1). The mean values of pH and EC were 8.06 and 17.62 mS/cm for surface soil-soluble salt, respectively, and the mean values of pH and EC were 8.10 (8.11) and 9.01 (6.35) mS/cm for the soil-soluble salt at 0–50 cm (50–100 cm) soil layer (Table S1).

The total cation concentrations ( $TZ^+ = K^+ + Na^+ + 2Ca^{2+} + 2Mg^{2+}$ ) of soil-soluble salt were greatly variable from 11 to 286 meq/L, while the total anion concentrations ( $TZ^- = Cl^- + NO_3^- + 2SO_4^{2-} + HCO_3^-$ ) changed between 10 and 179 meq/L in the water-level fluctuation zone of the lower Jinsha River (Table S1). Most of the soil samples had a higher  $TZ^+$  than  $TZ^-$ , and only a few samples had normalized inorganic charge balance (NICB) values within a 5% error (Table S1). The observed imbalance between  $TZ^+$  and  $TZ^-$  was probably caused by unmeasured  $PO_4^{3-}$  in the soil samples because phosphorus is an important element that contributes to soil fertility [32,33].  $Na^+$  and  $Ca^{2+}$  are the main cations, while  $SO_4^{2-}$  and  $HCO_3^-$  are the dominant anions in soil-soluble salt, following the order of  $SO_4^{2-} > HCO_3^- > Ca^{2+} > Cl^- > Na^+ > NO_3^- > Mg^{2+} > K^+$  (Figure 2).  $Na^+$ ,  $Ca^{2+}$ ,  $SO_4^{2-}$ , and  $HCO_3^-$  account for 78% of the total ions for soil-soluble salt in the WDDR and for 76% of the total ions for the soil-soluble phase in the BHTR (Table 1). The

chemical type of soil-soluble salt in the WDDR is Ca-Mg-Na-SO<sub>4</sub>-HCO<sub>3</sub>, which is similar to the soil-soluble salt in the BHTR with the type of Ca-Na-Mg-SO<sub>4</sub>-HCO<sub>3</sub> (Figure 3). Similar to the EC variation characteristics, the ion concentrations of the soil-soluble salt gradually decreased from the surface to the bottom of the soil profiles. There was less soil water content but higher ion concentrations in surface soils than in the deep soils in the lower Jinsha River Basin (Table S1). The ion distribution in the soil profiles was similar for all the major ions, i.e., the gradual decrease from the surface to the bottom of the soil profiles (Figure 4). Higher ion concentrations in surface soil samples show that it could be influenced by ionic enrichment and human activities. For the surface soil samples, the soils in the WDDR had higher Ca<sup>2+</sup> and HCO<sub>3</sub><sup>-</sup> than those in the BHTR, while the soils at the BHTR had higher K<sup>+</sup>, Cl<sup>-</sup> and SO<sub>4</sub><sup>2-</sup> than those in the WDDR (Table S1). The variation in the depth of ion concentrations for soil samples during 0–50 cm was significantly different from the soils in the WDDR and the BHTR, while the ion concentration variation in samples at the 50–100 cm soil layer in the WDDR was very similar to the soils in the BHTR (Table S1 and Figure 4).

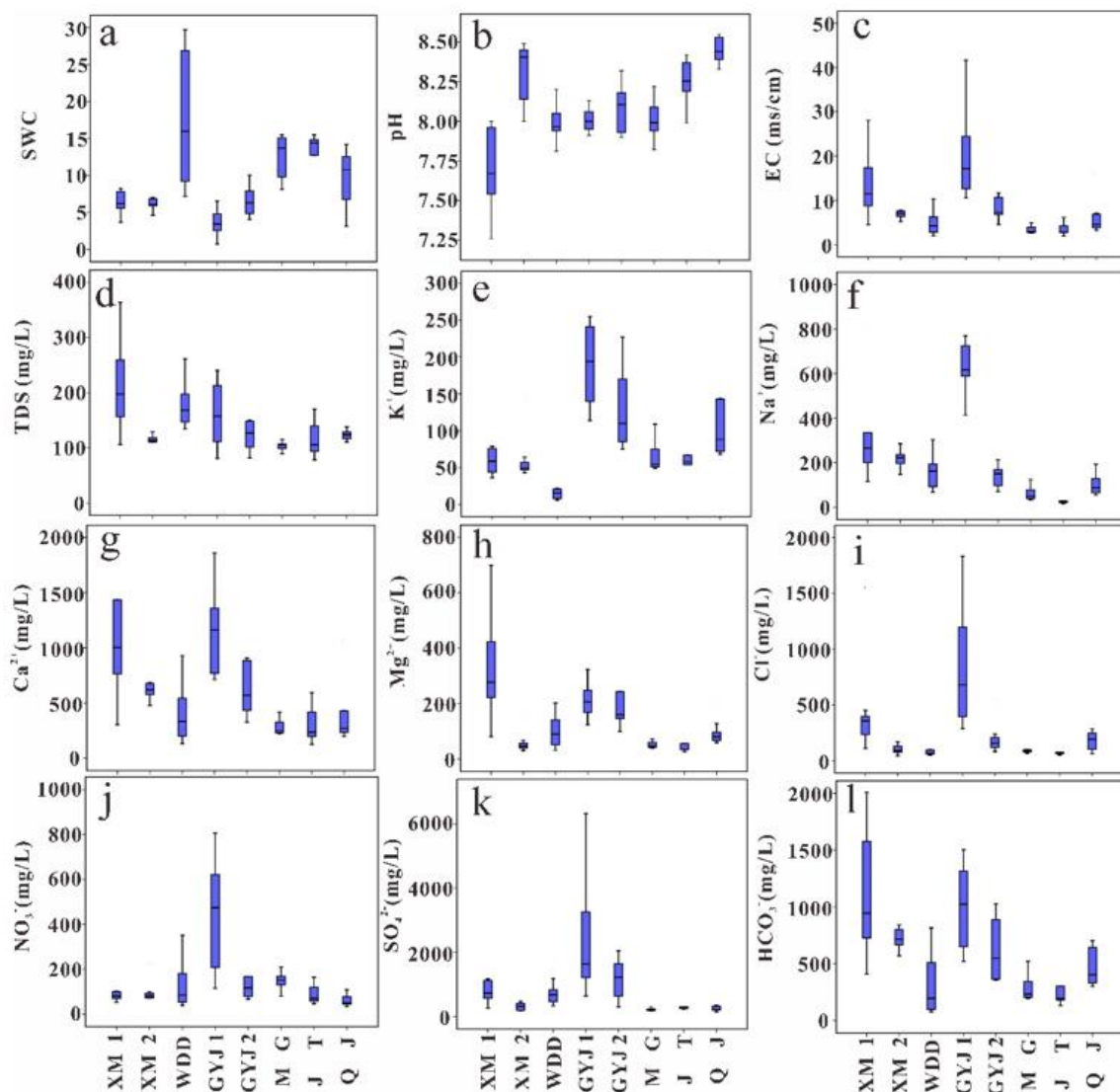


**Figure 2.** Boxplots for chemical composition of soil-soluble salt ((a) is for soil water content, (b) is for pH, (c) is for EC, (d) is for TDS, and (e–l) are for K<sup>+</sup>, Na<sup>+</sup>, Ca<sup>2+</sup>, Mg<sup>2+</sup>, Cl<sup>-</sup>, NO<sub>3</sub><sup>-</sup>, SO<sub>4</sub><sup>2-</sup>, and HCO<sub>3</sub><sup>-</sup>, respectively).

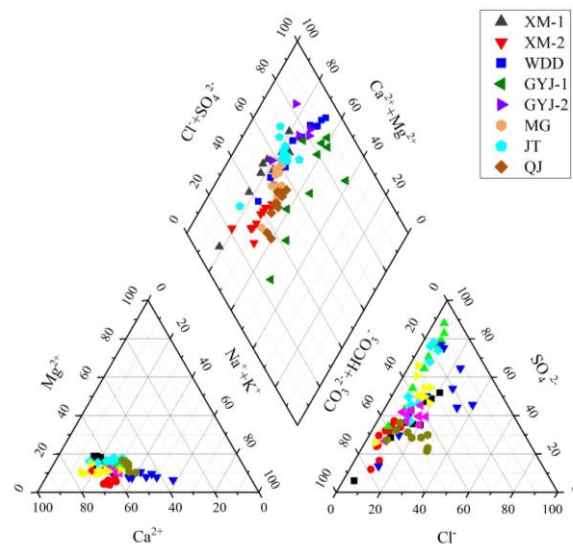


Figure 3. Piper diagrams of soil-soluble salt in the study area.

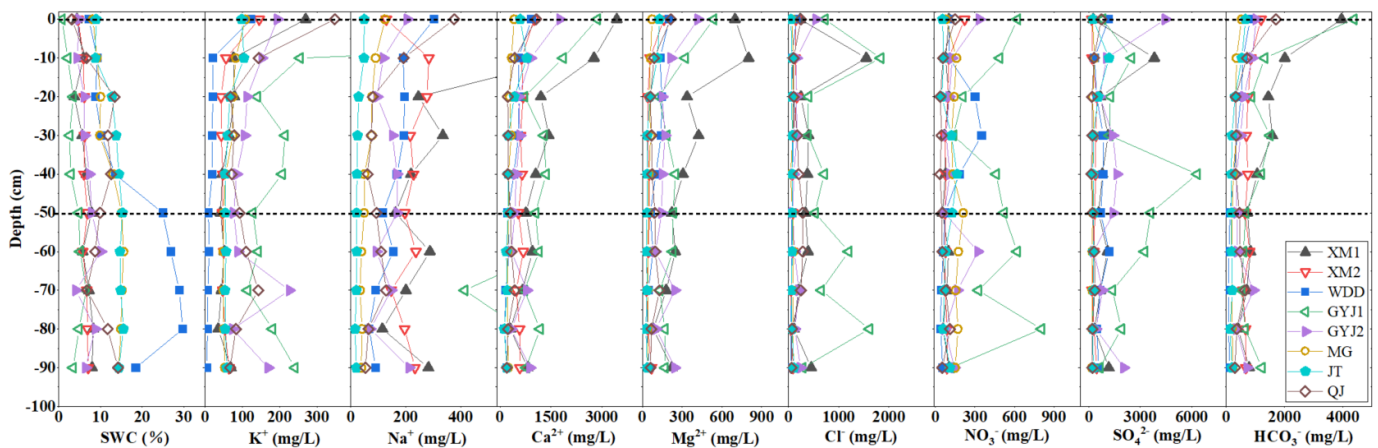


Figure 4. The soil water content and major ions distribution of soil-soluble salt.

There is a similar variation trend for hydrochemistry characteristics in soil-soluble salt from upstream to downstream for the WDDR and BHTR (Figure 2). The soil water content gradually increased from upstream to downstream except for the WDD soil profile in the lower Jinsha River Basin (Figure 2a). Affected by human activities, the ions in the soil-soluble salt of the ecological restoration areas are higher than the soil-soluble phase of the natural recovery areas. In detail,  $K^+$  in the XM1, XM2, GYJ1, and GYJ2 soil profiles have higher values than other soil profiles, and the  $K^+$  in soils of the BHTR is higher than those in the WDDR.  $Na^+$ ,  $Ca^{2+}$ , and  $Mg^{2+}$  are also higher in soil-soluble salt from the XM1, XM2, GYJ1, and GYJ2, while the soils contain more  $Na^+$  in the WDDR than those in the BHTR. Except for the  $HCO_3^-$  in the soil-soluble salt that has small differences between soils in the WDDR and the BHTR,  $Cl^-$ ,  $NO_3^-$  and  $SO_4^{2-}$  are all higher in the BHTR, especially for the GYJ1 and GYJ2 soil profiles (Figure 2e–l). Precipitation, rock weathering, and anthropogenic activities could release ions into soil-soluble salt during the processes of rainfall infiltration and water-rock interactions. The TDS values varied from 100 to 1000 mg/L while the molar ratios of  $Na^+ / Na^+ + Ca^{2+}$  and  $Cl^- / Cl^- + HCO_3^-$  were less than 0.5 for most soil samples (Figure 5), indicating that rock weathering can be identified as a main process for determining the chemistry composition of soil-soluble salt in the water-level fluctuation zone of the lower Jinsha River Basin.

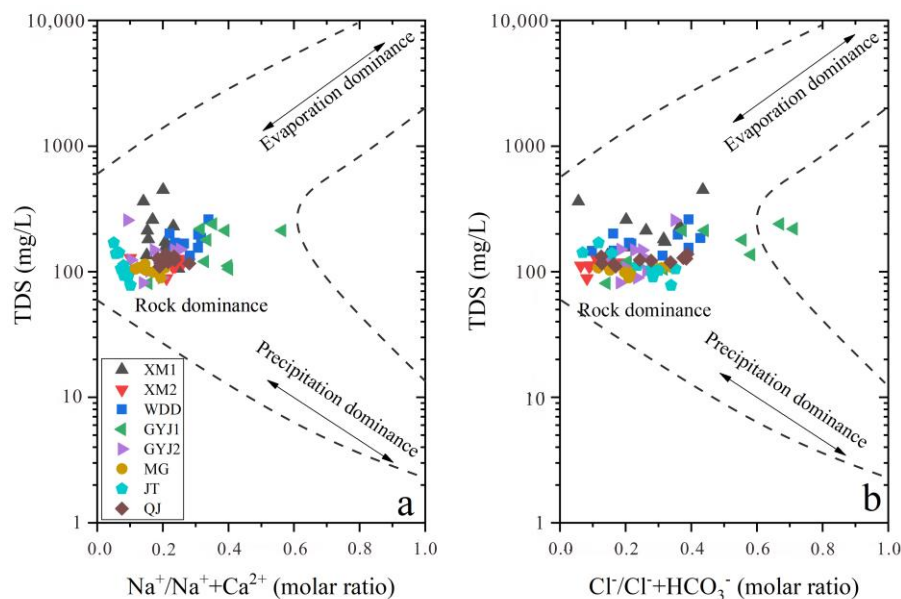


Figure 5. The Gibbs plots for chemical components in soil-soluble salt of soil profiles.

5. Discussion

5.1. The Distribution Characteristics of Major Ions in Soil-Soluble Salt

Although the WDDR and BHTR both belong to the dry-hot valley, the evaporation intensity is significantly higher in the WDDR. Therefore, SWC is lower in the WDDR than that in the BHTR. Similar to the SWC, the soil pH also increases from the upstream to downstream lower Jinsha River Basin, and the soils in the ecological restoration areas have a relatively lower pH (Figure 2b). The ion concentrations in soil-soluble salt decrease when the soil water content increases, and they have a significantly negative correlation coefficient between the two (Table 2). Furthermore, the ions show a gradually decreasing trend for soil-soluble salt in the soil profiles from upstream to downstream of the lower Jinsha River Basin (Figure 2e–l). The ion distribution from upstream to downstream of the WDDR and the BHTR shows that the ions in soil-soluble salt should originate from similar sources. The rock weathering could release more cations into soils in the WDDR, while ions in soils from the BHTR are mainly affected by anthropogenic factors such as agricultural activities and sewage discharge [34].

Table 2. Correlation coefficients between major components in soil-soluble salt in the study area.

WDDR	SWC	pH	EC	K <sup>+</sup>	Na <sup>+</sup>	Ca <sup>2+</sup>	Mg <sup>2+</sup>	Cl <sup>-</sup>	NO <sub>3</sub> <sup>-</sup>	SO <sub>4</sub> <sup>2-</sup>	HCO <sub>3</sub> <sup>-</sup>	BHTR
SWC	1	0.187	-0.803 **	-0.409 **	-0.643 **	-0.788 **	-0.812 **	-0.572 **	-0.487 **	-0.577 **	-0.691 **	SWC
pH	-0.041	1	-0.135	0.055	-0.243	-0.144	-0.117	-0.214	-0.354 *	-0.227	0.009	pH
EC	-0.506 **	-0.521 **	1	0.717 **	0.759 **	0.973 **	0.921 **	0.698 **	0.732 **	0.670 **	0.880 **	EC
K <sup>+</sup>	-0.500 **	-0.241	0.774 **	1	0.258	0.717 **	0.672 **	0.261	0.429 **	0.071	0.908 **	K <sup>+</sup>
Na <sup>+</sup>	-0.450 *	-0.330	0.923 **	0.620 **	1	0.624 **	0.540 **	0.806 **	0.637 **	0.804 **	0.478 **	Na <sup>+</sup>
Ca <sup>2+</sup>	-0.470 **	-0.477 **	0.991 **	0.805 **	0.921 **	1	0.951 **	0.690 **	0.703 **	0.617 **	0.876 **	Ca <sup>2+</sup>
Mg <sup>2+</sup>	-0.344	-0.675 **	0.953 **	0.617 **	0.875 **	0.921 **	1	0.588 **	0.606 **	0.634 **	0.830 **	Mg <sup>2+</sup>
Cl <sup>-</sup>	-0.267	-0.467 **	0.707 **	0.204	0.779 **	0.654 **	0.793 **	1	0.836 **	0.580 **	0.406 **	Cl <sup>-</sup>
NO <sub>3</sub> <sup>-</sup>	-0.209	0.089	0.064	0.051	-0.023	0.008	0.014	-0.096	1	0.612 **	0.472 **	NO <sub>3</sub> <sup>-</sup>
SO <sub>4</sub> <sup>2-</sup>	0.014	-0.407 *	0.506 **	-0.005	0.647 **	0.456 **	0.652 **	0.902 **	-0.054	1	0.274	SO <sub>4</sub> <sup>2-</sup>
HCO <sub>3</sub> <sup>-</sup>	-0.532	-0.422 **	0.944 **	0.890 **	0.818 **	0.961 **	0.834 **	0.452 *	-0.01	0.205	1	HCO <sub>3</sub> <sup>-</sup>

Note(s): \* Correlation is significant at the 0.05 level (2-tailed). \*\* Correlation is significant at the 0.01 level (2-tailed).

Due to extreme evaporation, the soil could lose more water and accumulate more salt on the surface in arid areas [35]. Although the climate is different from the arid areas, the evaporation intensity is still stronger in the lower Jinsha River Basin. Therefore, salt accumulation such as Cl<sup>-</sup> and SO<sub>4</sub><sup>2-</sup> occurs in soils from the WDDR and the BHTR. Some researchers have considered the maximum evaporation depth to be less than 50 cm in arid areas and the soil water below 50 cm depth, which is unaffected by evaporation [36]. In this way, the soil-soluble salt in the 0–50 cm soil layer could be influenced by precipitation

infiltration and slightly strong evaporation so that the soil water content and the ion concentrations would be relatively low in these soils. The soils in 50–100 cm have a high soil water content because they suffer from a weak evaporation effect, and more water can be stored in this soil layer. In addition, some ion concentrations are higher in the 0–50 cm soil layer while others have higher values in the 50–100 cm soil layer, indicating that the ion composition in soil-soluble salt could be influenced by multiple sources. For example, the soil ions in 0–50 cm can be affected by the precipitation and water-rock interaction, while the soils ions in 50–100 cm mainly originate from rock weathering. In conclusion, the ions in surface soils originate from complex sources (e.g., precipitation, anthropogenic activities, and rock weathering), while the ions in deep soils from the soil profiles are mainly influenced by water-rock interaction or silicate and carbonate weathering in the water-level fluctuation zone of the lower Jinsha River Basin.

### 5.2. The Major Ion Sources of Soil-Soluble Salt

Generally, the ion concentration of soil water in the water-level fluctuation zone can be influenced by altitude, soil texture, soil water content, and vegetation coverage [37]. The correlation coefficients among ions in soil-soluble salt in the WDDR and the BHTR were calculated to determine the relationships between ionic species and to identify the potential sources of ions (Table 2).  $\text{Na}^+$  and  $\text{Cl}^-$  of soil-soluble salt are well correlated with each other, and the correlation coefficient was larger than 0.80, suggesting they had similar sources. In general,  $\text{Na}^+$  exists in seawater, halite, and silicate rocks, while  $\text{Cl}^-$  can originate from seawater, halite, or anthropogenic inputs [38]. There are more  $\text{Na}^+$  than  $\text{Cl}^-$  for most soil samples (Figure 6a), implying that the silicate weathering or cation exchange could be the main source of  $\text{Na}^+$  in the soil-soluble salt of the water-level fluctuation zone in this region. The molar ratios of  $\text{Ca}^{2+} + \text{Mg}^{2+}$  and  $\text{SO}_4^{2-} + \text{HCO}_3^-$  were plotted near the 1:1 line (Figure 6b), suggesting that the ions of soil-soluble salt could be influenced by carbonate, silicate, and sulfate minerals [29]. The soil-soluble salt is also influenced by human activities such as domestic sewage discharge and fertilization because the  $\text{SO}_4^{2-}/\text{Na}^+$  and  $\text{NO}_3^-/\text{Na}^+$  ratios were high for some soils (Figure 6d). In addition, there is a positive correlation among  $\text{Cl}^-$ ,  $\text{NO}_3^-$  and  $\text{SO}_4^{2-}$  (Table 2), but automobile exhaust and chemical emissions are relatively few in the water-level fluctuation zone of the lower Jinsha River Basin, suggesting that these ions could come from refuse incineration or biomass burning.

The major cations ( $\text{K}^+$ ,  $\text{Na}^+$ ,  $\text{Ca}^{2+}$ ,  $\text{Mg}^{2+}$ ) have good correlations in soil-soluble salt, showing a roughly common source. These cations are generally common constituents of soil dust, so the main cations of soil-soluble salt should be influenced by mineral weathering. Many sources can contribute  $\text{K}^+$  for soil-soluble salts, such as sylvites, silicates, and agricultural activities [38]. The potential sources of soil-soluble  $\text{K}^+$  include the silicate weathering and burning of straw and fertilization in the water-level fluctuation zone of the lower Jinsha River Basin.  $\text{Mg}^{2+}$  mainly originates from carbonates, evaporite ( $\text{MgCO}_3$  and  $\text{MgSO}_4$ ), and Mg-containing minerals [38]. The  $\text{Mg}^{2+}/\text{Ca}^{2+}$  ratios of soil-soluble salt are all lower than 0.5 (Figure 6f), indicating that the  $\text{Mg}^{2+}$  in soil-soluble salt is mainly from carbonate dissolution in this region.  $\text{Ca}^{2+}$  is a common constituent of soil dust in limited water regions, and soil dust contains abundant carbonates with some gypsum [39]. Figure 6f shows that most of the soil samples are plotted in the region with an  $\text{SO}_4^{2-}/\text{Ca}^{2+}$  molar ratio of less than one, showing that  $\text{Ca}^{2+}$  in soil-soluble salt originates from carbonates weathering in the lower Jinsha River Basin. This correlation was extremely high for  $\text{Ca}^{2+}$  and  $\text{HCO}_3^-$  in soil-soluble salt (Table 2), suggesting that calcite and carbonates could dissolve these ions more into soil-soluble salt in this region. Furthermore, the average value of  $\text{Ca}^{2+}/\text{Na}^+$  and  $\text{Mg}^{2+}/\text{Na}^+$  were 2.5 and 0.87, respectively, which is similar to the silicates but much lower than the carbonates (Figure 6e). These results show that the  $\text{Na}^+$  in soil-soluble salt was controlled by the silicate weathering, while  $\text{Ca}^{2+}$  and  $\text{Mg}^{2+}$  mainly came from the carbonate dissolution.

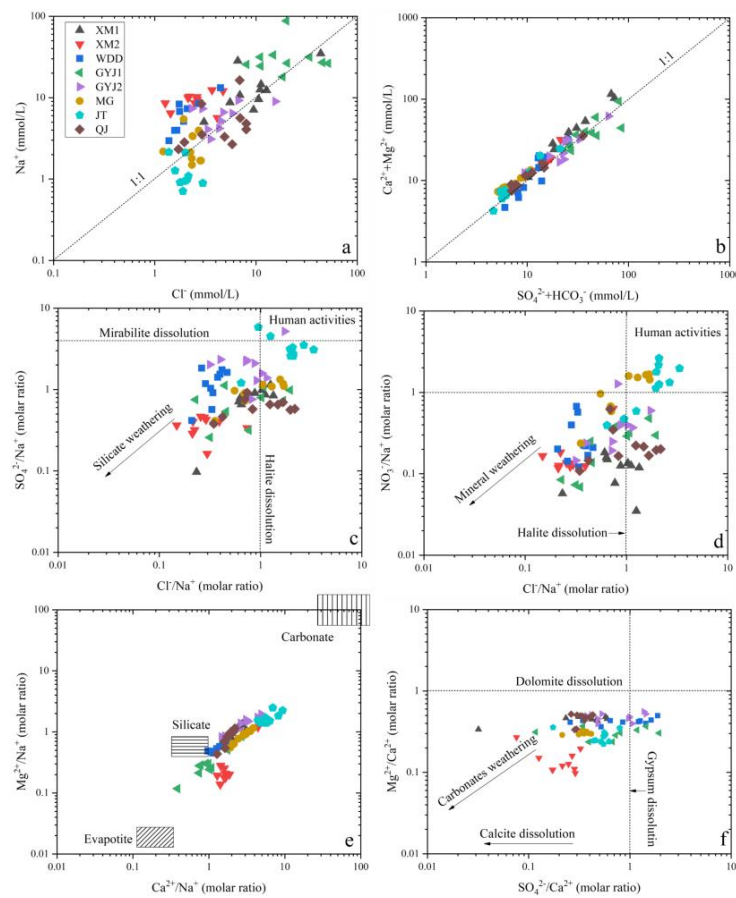


**Figure 6.** Major ions pairs of soil-soluble salt from the soil profiles ((a) is for  $\text{Na}^+$  vs.  $\text{Cl}^-$ , (b) is for  $\text{Ca}^{2+} + \text{Mg}^{2+}$  vs.  $\text{SO}_4^{2-} + \text{HCO}_3^-$ , (c) is for  $\text{SO}_4^{2-} / \text{Na}^+$  vs.  $\text{Cl}^- / \text{Na}^+$ , (d) is for  $\text{NO}_3^- / \text{Na}^+$  vs.  $\text{Cl}^- / \text{Na}^+$ , (e) is for  $\text{Mg}^{2+} / \text{Na}^+$  vs.  $\text{Ca}^{2+} / \text{Na}^+$ , and (f) is for  $\text{Mg}^{2+} / \text{Ca}^{2+}$  vs.  $\text{SO}_4^{2-} / \text{Ca}^{2+}$ , respectively).

Most soil samples have negative values for CAI-1 and CAI-2 (Figure 7), indicating that excess  $\text{Ca}^{2+}$  could be transferred into  $\text{Na}^+$  based on the process of mineral dissolution and weathering in the soil samples [31]. Considering the high concentrations of  $\text{Ca}^{2+}$  in the soil-soluble salt and strong chemical weathering, the cation exchange could take place in the soils of the lower Jinsha River Basin.

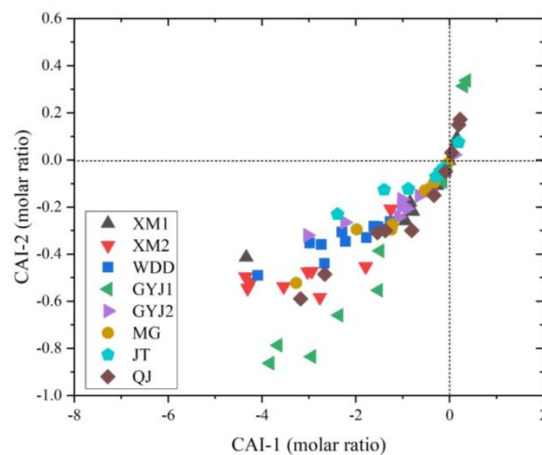


**Figure 7.** Plots of CAI-1 and CAI-2 of soil-soluble salt from the soil profiles.

The soil samples in different depths of soil profiles corresponded to different total data variances. For the surface soil samples, the first factor (PC1) explained 78.06% and

77.18% of the total variance, respectively, for the soils in the WDDR and the BHTR. PC1 was characterized by high concentrations of major ions except for  $\text{NO}_3^-$  and  $\text{SO}_4^{2-}$  (Table 3), showing the silicate weathering controls on the soil-soluble phase chemistry in the WDDR. The second factor (PC2) accounted for 21.94% of the total variance and is characterized by a high concentration of  $\text{Na}^+$  and  $\text{Cl}^-$ , while low concentrations of other ions (Table 3) imply that precipitation can recharge the surface soils in the WDDR. The PC1 and PC2 are 77.18% and 14.28% for the surface soils in the BHTR (Table 3); high concentrations of major ions in PC1 and higher  $\text{Mg}^{2+}$ ,  $\text{Cl}^-$ , and  $\text{SO}_4^{2-}$  in PC2 show that much stronger mineral weathering happened in the BHTR. For the soil-soluble salt in 0–50 cm soil layers in the WDDR, the PC1 explains 71.36% of the total variance and is characterized by the high concentration of all the total ion concentrations except for  $\text{NO}_3^-$  while the PC2 is characterized by lower  $\text{K}^+$  and  $\text{HCO}_3^-$  (Table 3), suggesting a mixed source influenced by mineral weathering and anthropogenic input. The PC1 and PC2 explain 75.47% and 8.7% of the total variance for soil-soluble salt in the BHTR, and the PC2 is characterized by high  $\text{Na}^+$ ,  $\text{Cl}^-$ ,  $\text{NO}_3^-$  and  $\text{SO}_4^{2-}$ , which implies that the ions in soil-soluble salt are also affected by human activities in the BHTR. The rock weathering (e.g., carbonate or/and silicate weathering) is much stronger for soil-soluble salt in the 50–100 cm soil layer because the cumulative value is 89.58% and 86.58%, respectively for the soil-soluble salt in the WDDR and BHTR (Table 3). In summary, the potential sources of major ions in soil-soluble salt are precipitation, rock weathering (silicate weathering and carbonate weathering), and anthropogenic input in the water-level fluctuation zone of the lower Jinsha River Basin.

**Table 3.** Physical and chemical parameters on two significant principal components for soil-soluble salt at different depths in the study area.

Location	Variation	Surface		0–50 cm		50–100 cm	
		PC1	PC2	PC1	PC2	PC1	PC2
WDDR	SWC	−0.589	0.808	−0.557	0.735	−0.836	0.410
	pH	−0.991	−0.137	−0.663	0.090	0.213	−0.906
	EC	1.000	−0.003	0.993	0.085	0.987	0.127
	$\text{K}^+$	0.993	−0.119	0.823	−0.506	0.907	−0.355
	$\text{Na}^+$	0.939	0.345	0.905	0.251	0.943	−0.056
	$\text{Ca}^{2+}$	1.000	−0.005	0.987	0.145	0.979	0.018
	$\text{Mg}^{2+}$	0.996	0.086	0.940	0.265	0.726	0.653
	$\text{Cl}^-$	0.991	0.136	0.929	0.313	0.766	0.599
	$\text{NO}_3^-$	−0.470	−0.883	−0.474	0.675	0.850	−0.129
	$\text{SO}_4^{2-}$	−0.451	0.892	0.858	0.483	0.231	0.826
	$\text{HCO}_3^-$	0.996	−0.090	0.967	−0.212	0.944	−0.261
	Variability (%)	78.057	21.943	71.364	16.343	65.149	24.427
	Cumulative (%)	78.057	100.000	71.364	87.708	65.149	89.576
BHTR	SWC	−0.939	−0.006	−0.874	0.334	−0.900	0.362
	pH	0.563	0.425	−0.532	0.561	−0.461	−0.482
	EC	0.995	−0.082	0.988	0.133	0.996	0.017
	$\text{K}^+$	0.885	−0.436	0.954	−0.139	0.825	−0.504
	$\text{Na}^+$	0.928	−0.243	0.823	0.403	0.930	0.158
	$\text{Ca}^{2+}$	0.984	0.061	0.961	−0.082	0.992	0.059
	$\text{Mg}^{2+}$	0.948	0.250	0.928	−0.134	0.915	−0.248
	$\text{Cl}^-$	0.953	0.249	0.817	0.101	0.800	0.364
	$\text{NO}_3^-$	0.970	−0.003	0.847	0.256	0.753	0.570
	$\text{SO}_4^{2-}$	0.270	0.936	0.823	0.433	0.855	0.292
	$\text{HCO}_3^-$	0.931	−0.360	0.920	−0.209	0.802	−0.557
	Variability (%)	77.179	14.279	75.473	8.695	72.392	14.191
	Cumulative (%)	77.179	91.458	75.473	84.168	72.392	86.583

### 5.3. The Source Contributions for Major Ions in Soil-Soluble Salt

The ions in soil-soluble salt mainly come from precipitation, anthropogenic activities (e.g., agriculture fertilization), silicate weathering, and carbonate weathering.

We used  $\text{Cl}^-$  to calculate the ions input into soil-soluble salt from atmospheric precipitation because it experiences less external interference [29]. We cited the data on precipitation in representative cities of the lower Jinsha River Basin for comparative analysis in this study [40]. The ion contributions are relatively low for precipitation, with a mean of 0.7% for soil-soluble salt in the water-level fluctuation zone of the lower Jinsha River Basin. The annual precipitation amount in the BHTR was higher than the WDDR, so more ions could be input into soil-soluble salt in the BHTR. In detail, the contribution of major ion inputs in soil-soluble salt originating from the precipitation has been calculated as 0.53% ( $\text{K}^+$ ), 0.65% ( $\text{Na}^+$ ), 0.8% ( $\text{Ca}^{2+}$ ), 0.66% ( $\text{Mg}^{2+}$ ), 1.01% ( $\text{NO}_3^-$ ) and 0.41% ( $\text{SO}_4^{2-}$ ), respectively.

Previous researchers showed that  $\text{Cl}^-$ ,  $\text{NO}_3^-$ ,  $\text{K}^+$ , and  $\text{Na}^+$  could be influenced by agricultural inputs, while  $\text{Ca}^{2+}$ ,  $\text{Mg}^{2+}$ , and  $\text{HCO}_3^-$  were considered to be insensitive to pollution [34]. Except for the precipitation and anthropogenic input, the  $\text{NO}_3^-$  in soil-soluble salt was almost unaffected by other factors. Therefore, we could calculate the  $\text{NO}_3^-$  from agricultural activities by the mass balance equation. The results show that the concentration of  $\text{NO}_3^-$  in soil-soluble salt that originated from an agricultural input was 101.8 mg/L and 175 mg/L, respectively, in the WDDR and the BHTR. Additionally, the molar ratios of  $\text{Cl}^-/\text{Na}^+$ ,  $\text{NO}_3^-/\text{Na}^+$ , and  $\text{K}^+/\text{Na}^+$  from the agricultural end-member were 5, 4, and 1.4, respectively [34]. Therefore, we could calculate the major ions that originated from anthropogenic activities. For example, the  $\text{K}^+$  in soil-soluble salt that originated from anthropogenic activities was 22.4 mg/L and 38.8 mg/L, respectively, for the WDDR and the BHTR. Similarly, the amount of  $\text{Na}^+$  and  $\text{Cl}^-$  input into soil-soluble salt from anthropogenic activities were 9.43 mg/L (16.3 mg/L) and 72.8 mg/L (126 mg/L), respectively, in the WDDR (or the BHTR). The mean contribution of the anthropogenic input for ions in soil-soluble salt was 29.3% and 54.6%, respectively, in the WDDR and the BHTR (Figure 8).

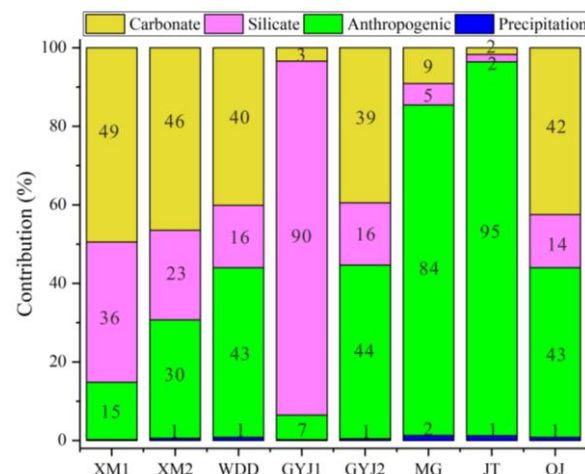


**Figure 8.** The percentage contribution of various ions sources for soil-soluble salt in the soil profiles.

Silicate weathering is also an important source for releasing  $\text{Na}^+$  and  $\text{K}^+$  into soils and can influence the ion component of soil-soluble salt. The ions in soil-soluble salt were mainly affected by the water-rock interaction, but the evaporation dominance was rare in the water-level fluctuation zone of the lower Jinsha River Basin (Figure 5). In other words, the  $\text{Na}^+$  and  $\text{K}^+$  in soil-soluble salt, except originating from precipitation and anthropogenic activities, could also be contributed by silicate weathering in this region. By this calculation, the ionic amount of  $\text{Na}^+$  was averaged for 224.6 mg/L and 207.5 mg/L, respectively, and for soil-soluble salt in the WDDR and the BHTR. The mean amount of  $\text{K}^+$  in soil-soluble salt from the silicate weathering was 31.6 mg/L and 125.4 mg/L, respectively, for soils collected

from the WDDR and the BHTR. The molar ratios of  $\text{Ca}^{2+}/\text{Na}^{+}$  and  $\text{Mg}^{2+}/\text{Na}^{+}$  in silicates were 0.6 and 0.4, respectively [41]. If the  $\text{Ca}^{2+}$  and  $\text{Mg}^{2+}$  can release into soil-soluble salt through silicate weathering, these ions in soil-soluble salt from the silicate weathering can be calculated by the relative ratios to the  $\text{Na}^{+}$  in silicates [29]. The results show that  $\text{Ca}^{2+}$  in soil-soluble salt that originates from the silicate weathering is about 134.8 mg/L and 124.5 mg/L, while the  $\text{Mg}^{2+}$  that comes from silicate weathering is 89.8 mg/L and 83 mg/L, respectively in soils collected from the WDDR and the BHTR. Using the ionic mass balance method, the ion contribution in soil-soluble salt from silicate weathering can be calculated for 31.7% to 47.7% with a mean of 41.3% in the WDDR and between 8% and 69.9% with a mean of 33.4% in the BHTR (Figure 8). In a similar way, we calculated the contribution of ions in soil-soluble salt that originated from carbonate weathering. The ionic proportion for soil-soluble salt from the carbonates accounted for 45.4% and 19.3%, respectively, in the WDDR and the BHTR (Figure 8).

In summary, the results indicate that the two main sources (water-rock interaction and anthropogenic activities) of major ions in soil-soluble salt contributed 54.2% and 45.1% of the total ions in soils, respectively. However, the precipitation contribution to soil was less than 1% in this region.

## 6. Conclusions

The hydrochemical composition of soil-soluble salt in the water-level fluctuation zone of the lower Jinsha River Basin was investigated for its ion distribution and sources in detail. The soil water content was about 10% and gradually increased from upstream to downstream, and the soil profiles in the ecological restoration had lower soil water content (5.68%) than that in natural recovery areas (13.37%) due to more plant growth impacts. The soil water content (only 5.24%) was also low in surface soils because it was affected by extreme evaporation, and it increased along the depth of the soil profile in the lower Jinsha River Basin.

The major ion composition of soil-soluble salt is comparable between the WDDR and the BHTR, characterized by the high concentration of  $\text{Na}^{+}$ ,  $\text{Ca}^{2+}$ ,  $\text{SO}_4^{2-}$ , and  $\text{HCO}_3^{-}$ , which accounted for more than 75% of the total ions. The chemical type of soil-soluble salt is Ca-Mg-Na- $\text{SO}_4$ - $\text{HCO}_3$  and Ca-Na-Mg- $\text{SO}_4$ - $\text{HCO}_3$ , respectively, in the WDDR and the BHTR. The major ion concentration of soil-soluble salt shows a gradually decreasing trend from upstream to downstream in the lower Jinsha River Basin. The soils collected from the ecological restoration areas have higher ion concentrations than that in the natural recovery area. More ion enrichment and salt accumulation were evident in the surface soils due to a strong evaporation effect, and the ion concentration of soil-soluble salt was higher in the shallow soil layer (<50 cm) than in the deep soil layer (>50 cm). The original sources for major ions in soil-soluble salt include precipitation, anthropogenic activities, and rock weathering in the water-level fluctuation zone of the lower Jinsha River Basin. Precipitation could affect the surface and shallow soil ions; anthropogenic activities are key for the ion composition of the surface soil-soluble salt, and silicate weathering and carbonate weathering can also release more ions ( $\text{Na}^{+}$  and  $\text{Ca}^{2+}$ ) into soil-soluble salt in the WDDR and the BHTR.

By using the mass balance method, the contribution of major ions in soil-soluble salt from various sources was calculated in this study. The order of the contribution rate from potential sources for the soil-soluble salt was as follows: rocks weathering (54.2%) > anthropogenic activities (45.1%) > precipitation input (0.7%). In detail, precipitation contributions were very small for ions in soil-soluble salt, which only accounted for 0.54% and 0.79%, respectively, in the WDDR and the BHTR. The contributions of human activities for major ions in soil-soluble salt were 29.3% and 54.6%, respectively, in the WDDR and the BHTR. The contribution of silicate weathering was comparable between soil-soluble salt collected from the WDDR and the BHTR, which contributed 24.8% and 25.4%, respectively. Carbonate weathering contributes more major ions in soil-soluble salt from the WDDR than that in the BHTR, and the contributions were 45.36% and 19.21%,

respectively. As a whole, the major ions in soil-soluble salt were mainly influenced by silicate weathering and carbonate weathering for soils in the WDDR, while human activities contributed more ions for soil-soluble salt in the BHTR.

This study not only reveals the major ion sources for soil-soluble salt in the water-level fluctuation zone of the lower Jinsha River Basin but also provides a useful reference for water resource management in the Jinsha River Basin.

**Supplementary Materials:** The following supporting information can be downloaded at: <https://www.mdpi.com/article/10.3390/w15071403/s1>, Table S1. The soil water content (SWC) and chemical composition of soil water in the water-level fluctuation zone of the lower Jinsha River Basin, where the unit of SWC is %, the unit of EC is mS/cm, and the unit of ionic concentration is mg/L.

**Author Contributions:** Funding acquisition, K.J.; methodology, Q.Z., J.Y. and H.Z.; project administration, Y.L.; software, D.W.; validation, C.Z.; formal analysis, Y.H.; writing—original draft preparation, K.J.; writing—review and editing, K.J. All authors have read and agreed to the published version of the manuscript.

**Funding:** This study was financially supported by the National Key R&D Program of China (Grant No. 2021YFE011900), the Fundamental Research Funds for Central Public Welfare Research Institutes (Grant No. CKSF2021464/CQ and CKSF2023299/CQ), the Knowledge Innovation Program of Wuhan-Shuguang (Grant No. 2022020801020245), and the Program of China Three Gorges Construction Engineering Corporation (Grant No. JG/19042B and JG/19043B).

**Data Availability Statement:** The study did not report any data.

**Acknowledgments:** Editor Allison Wu and anonymous reviewers are sincerely acknowledged for their invaluable comments.

**Conflicts of Interest:** The authors declare no conflict of interest.

## References

1. Yinglan, A.; Wang, G.; Liu, T.; Xue, B.; Kuczera, G. Spatial variation of correlations between vertical soil water and evapotranspiration and their controlling factors in a semi-arid region. *J. Hydrol.* **2019**, *574*, 53–63.
2. De Queiroz, M.G.; da Silva, T.G.F.; Zolnier, S.; Jardim, A.M.; Souza, C.A.A.; Júnior, G.; Morais, J.E.F.; Souza, L.S.B. Spatial and temporal dynamics of soil moisture for surfaces with a change in land use in the semi-arid region of Brazil. *Catena* **2020**, *188*, 104457. [[CrossRef](#)]
3. Xu, D.; Han, J.J.; Zhao, Y.Y. Characterization of soil water by the means of hydrogen and oxygen isotope ratio at dry-wet season under different soil layers in the dry-hot valley of Jinsha River. *Open Chem.* **2020**, *18*, 822–832. [[CrossRef](#)]
4. Li, Z.C.; Zhao, Y.Y.; Wang, K.Q.; Duan, X.; Xu, G.Q. Soil preferential flow characteristics in active and stable gully catchment areas of the Dry-hot Valleys of the Jinsha River (in Chinese with English abstract). *J. Soil Water Conserv.* **2022**, *36*, 119–127.
5. Bao, Y.; He, X.; Wen, A.; Gao, P.; Tang, Q.; Yan, D.; Long, Y. Dynamic changes of soil erosion in a typical disturbance zone of China's Three Gorges Reservoir. *Catena* **2018**, *169*, 128–139. [[CrossRef](#)]
6. Li, Y.Y.; Gao, B.; Xu, D.Y.; Lu, J.; Zhou, H.D.; Gao, L. Heavy metals in the water-level-fluctuation zone soil of the three Gorges Reservoir, China: Remobilization and catchment-wide transportation. *J. Hydrol.* **2022**, *612*, 128108. [[CrossRef](#)]
7. Xiao, H.; Guo, P.; Zhang, Q.H.; Hu, H.; Hong, H.; Zhang, L.; Yang, Y.S.; Xia, Z.Y.; Li, M.Y.; Kang, H.L.; et al. Variation in soil properties and its influence on the dynamic change of soil erosion resistance to overland flow in the water-level fluctuation zone of the Three Gorges Reservoir, China. *Catena* **2022**, *213*, 106141. [[CrossRef](#)]
8. Han, J.J.; Duan, X.; Zhao, Y.Y.; Xiong, H.Q. Spatial and temporal variability of soil moisture on sloping lands of different land use types in a Dry-hot Valley (in Chinese with English abstract). *J. Soil Water Conserv.* **2017**, *31*, 129–136.
9. Yue, X.W.; Fang, H.D.; Qian, K.J.; Ji, Z.H.; Yang, Y.X.; Pan, Z.X.; Peng, H.; Fang, J.; Kui, J.L. Effect of different land use on soil moisture in Dry-hot Valley of Jinsha River (in Chinese with English abstract). *J. Anhui Agric. Sci.* **2010**, *38*, 14963–14965.
10. Han, J.L.; Duan, X.; Zhao, Y.Y. Spatial and temporal variability of soil moisture on slope land of different vegetation of dry-hot valley in Jinsha River (in Chinese with English abstract). *Arid Land Geogr.* **2019**, *42*, 121–130.
11. Wu, H.; Xiong, D.H.; Zhang, B.J.; Guo, M.; Yang, D.; Zhang, S.; Xiao, L.; Fang, H.D. Spatial and temporal change of soil water in different sections of Gully in Dry-hot Valley region of Southwest China (in Chinese with English abstract). *Southwest China J. Agric. Sci.* **2018**, *31*, 384–392.
12. Wang, Y.D.; Zhang, M.Y.; Fan, J.C.; He, G.X.; Zhang, M.Z.; Fang, H.D. Soil Moisture of *Leucaena leucocephala* Plantations in the Dry-hot Valley of Jinsha River, Yunnan (in Chinese with English abstract). *J. Trop. Biol.* **2018**, *9*, 61–69.

13. Hou, L.Z.; Wang, X.S.; Hu, B.X.; Shang, J.; Wang, L. Experimental and numerical investigations of soil water balance at the hinterland of the Badain Jaran Desert for groundwater recharge estimation. *J. Hydrol.* **2016**, *540*, 386–396. [[CrossRef](#)]
14. Huang, D.W.; Chen, J.S.; Zhan, L.C.; Wang, T.; Su, Z.G. Evaporation from sand and loess soils: An experimental approach. *Transp. Porous Media* **2016**, *113*, 639–651. [[CrossRef](#)]
15. Han, D.M.; Zhou, T.T. Soil water movement in the unsaturated zone of an inland arid region: Mulched drip irrigation experiment. *J. Hydrol.* **2018**, *559*, 13–29. [[CrossRef](#)]
16. Rao, W.B.; Zheng, F.; Tan, H.; Yong, B.; Jin, K.; Wang, S.; Zhang, W.B.; Chen, T.Q.; Wang, Y.N. Major ion chemistry of a representative river in South-central China: Runoff effects and controlling mechanisms. *J. Hazard. Mater.* **2019**, *378*, 120755. [[CrossRef](#)] [[PubMed](#)]
17. Shen, H.G.; Rao, W.B.; Tan, H.B.; Guo, H.Y.; Ta, W.Q.; Zhang, X.Y. Controlling factors and health risks of groundwater chemistry in a typical alpine watershed based on machine learning methods. *Sci. Total Environ.* **2023**, *854*, 158737. [[CrossRef](#)]
18. Jin, L.X.; Andrews, D.M.; Holmes, G.H.; Lin, H.; Brantley, S.L. Opening the “Black Box”: Water chemistry reveals hydrological controls on weathering in the Susquehanna shale hills critical zone observatory. *Vadose Zone J.* **2011**, *10*, 928–942. [[CrossRef](#)]
19. Pan, F.; Ma, J.Z.; Zhou, X.Y.; Edmunds, W.M.; Gates, G.B. Geostatistical characterization of soil moisture and chloride distribution in deep vadose profiles of the Badain Jaran Desert, Northwestern China. *Environ. Earth Sci.* **2013**, *70*, 977–991. [[CrossRef](#)]
20. Tan, H.B.; Liu, Z.H.; Rao, W.B.; Wei, H.Z.; Zhang, Y.D.; Jin, B. Stable isotopes of soil water: Implications for soil water and shallow groundwater recharge in hill and gully regions of the Loess Plateau, China. *Agric. Ecosyst. Environ.* **2017**, *243*, 1–9. [[CrossRef](#)]
21. Jin, K.; Rao, W.B.; Wang, S.; Zhang, W.B.; Zheng, F.W.; Li, T.N.; Lu, Y.; Zhang, Q.Z. Stable isotopes ( $\delta^{18}\text{O}$  and  $\delta^2\text{H}$ ) and chemical characteristics of soil solution in the unsaturated zone of an arid desert. *J. Radioanal. Nucl. Chem.* **2021**, *330*, 367–380. [[CrossRef](#)]
22. Liu, S.W.; Zhang, X.F.; Xu, Q.X.; Liu, D.C.; Yuan, J.; Wang, M.L. Variation and driving factors of water discharge and sediment load in different regions of the Jinsha River Basin in China in the past 50 years. *Water* **2019**, *11*, 1109. [[CrossRef](#)]
23. Wu, H.; Xiong, D.; Xiao, L.; Zhang, S.; Yuan, Y.; Su, Z.A.; Zhang, B.J.; Yang, D. Effects of vegetation coverage and seasonal change on soil microbial biomass and community structure in the dry-hot valley region. *J. Mountain Sci.* **2018**, *15*, 1546–1558. [[CrossRef](#)]
24. Hu, Y.; Lu, Y.; Jin, K.; Zhou, H.M.; Wan, D.; Zhang, Q.Z.; Yan, J.M. Discussion on ecological restoration in Dry-hot Valley (in Chinese with English abstract). *J. Yangtze River Sci. Res. Inst.* **2021**, *38*, 69–75.
25. Wan, D.; Zhou, H.M.; Lu, Y.; Jin, K.; Yu, J.; Zhang, Q.Z.; Hu, Y.; Yan, J.M. Progress and perspective of vegetation restoration in Water-level-fluctuating zone of Dry-hot Valley reservoirs in Jinsha River (in Chinese with English abstract). *Ecol. Environ. Monit. Three Gorges* **2021**, *6*, 9–21.
26. Lin, Y.M.; Chen, A.M.; Yan, S.W.; Rafay, L.; Du, K.; Wang, D.J.; Ge, Y.G.; Li, J. Available soil nutrients and water content affect leaf nutrient concentrations and stoichiometry at different ages of *Leucaena leucocephala* forests in dry-hot valley. *J. Soils Sediments* **2019**, *19*, 511–521. [[CrossRef](#)]
27. Piper, A.M. A graphic procedure in the geochemical interpretation of water-analyses. *Eos Trans. Am. Geophys. Union* **1944**, *25*, 914–928. [[CrossRef](#)]
28. Gibbs, R.J. Mechanisms controlling world water chemistry. *Science* **1971**, *172*, 870–872. [[CrossRef](#)]
29. Li, Y.Z.; Gao, Z.J.; Liu, J.T.; Wang, M.; Han, C. Hydrogeochemical and isotopic characteristics of spring water in the Yarlung Zangbo River Basin, Qinghai-Tibet Plateau, Southwest China. *J. Mt. Sci.* **2021**, *18*, 2061–2078. [[CrossRef](#)]
30. Zhu, B.Q.; Yang, X.P.; Rioual, P.; Qin, X.G.; Liu, Z.T.; Xiong, H.G.; Yu, J.J. Hydrogeochemistry of three watersheds (the Erlqis, Zhungarar and Yili) in northern Xinjiang, NW China. *Appl. Geochem.* **2011**, *26*, 1535–1548. [[CrossRef](#)]
31. Li, P.; Wu, J.; Qian, H.; Zhang, Y.; Yang, N.; Jing, L.; Yu, P. Hydrogeochemical characterization of groundwater in and around a wastewater irrigated forest in the southeastern edge of the Tengger Desert, northwest China. *Expo. Health* **2016**, *8*, 331–348. [[CrossRef](#)]
32. Chen, Z.L.; Fang, F.; Shao, Y.; Jiang, Y.X.; Huang, J.J.; Guo, J.S. The biotransformation of soil phosphorus in the water level fluctuation zone could increase eutrophication in reservoirs. *Sci. Total Environ.* **2021**, *763*, 142976. [[CrossRef](#)]
33. Wang, S.; Rao, W.B.; Qian, J.; Mao, C.P.; Li, K. Phosphorus species in bottom sediments of the Three Gorges Reservoir during low and high water level periods. *Environ. Sci. Pollut. Res.* **2020**, *27*, 17923–17934. [[CrossRef](#)]
34. Chetelat, B.; Liu, C.Q.; Zhao, Z.Q.; Wang, Q.L.; Li, S.L.; Li, J.; Wang, B.L. Geochemistry of the dissolved load of the Changjiang Basin rivers: Anthropogenic impacts and chemical weathering. *Geochim. Cosmochim. Acta* **2008**, *72*, 4254–4277. [[CrossRef](#)]
35. Chen, J.S.; Sun, X.X.; Gu, W.Z.; Tan, H.B.; Rao, W.B.; Dong, Z.; Liu, X.Y.; Su, Z.G. Isotopic and hydrochemical data to restrict the origin of the groundwater in the Badain Jaran Desert, North China. *Geochem. Int.* **2012**, *50*, 455–465. [[CrossRef](#)]
36. Zhao, J.B.; Ma, Y.D.; Luo, X.Q.; Yue, D.P.; Shao, T.J.; Dong, Z.B. The discovery of surface runoff in the megadunes of Badain Jaran Desert, China, and its significance. *Sci. China Earth Sci.* **2017**, *60*, 707–719. [[CrossRef](#)]
37. Zhang, L.M.; Huangpu, C.H.; Yuan, Y.S.; Meng, Y.Y.; Jia, X. The correlations between vegetation composition and soil characteristics in the riparian zone of Shengjin Lake (in Chinese with English abstract). *Pratacultural Sci.* **2021**, *38*, 52–62.
38. Rao, W.B.; Han, G.Y.; Tan, H.B.; Jin, K.; Wang, S.; Chen, T.Q. Chemical and Sr isotopic characteristics of rainwater on the Alxa Desert Plateau, North China: Implication for air quality and ion sources. *Atmos. Res.* **2017**, *193*, 163–172. [[CrossRef](#)]
39. Rao, W.B.; Chen, J.; Yang, J.D.; Ji, J.F.; Zhang, G.X. Sr isotopic and elemental characteristics of calcites in the Chinese deserts: Implications for eolian Sr transport and seawater Sr evolution. *Geochim. Cosmochim. Acta* **2009**, *73*, 5600–5618. [[CrossRef](#)]

40. Wang, D.X.; Li, Y.P.; Chen, Y.; Zhou, S.C. Study on the change trend and ion characteristics of atmospheric precipitation in Kunming from 2015 to 2019 (in Chinese with English abstract). *Environ. Sci. Surv.* **2021**, *40*, 47–51.
41. Chatterjee, J.; Singh, S.K.  $^{87}\text{Sr}/^{86}\text{Sr}$  and major ion composition of rainwater of Ahmedabad, India: Sources of base cations. *Atmos. Environ.* **2012**, *63*, 60–67. [[CrossRef](#)]

**Disclaimer/Publisher's Note:** The statements, opinions and data contained in all publications are solely those of the individual author(s) and contributor(s) and not of MDPI and/or the editor(s). MDPI and/or the editor(s) disclaim responsibility for any injury to people or property resulting from any ideas, methods, instructions or products referred to in the content.